A novel method of reconstruction for weak-phase optical interferometry

Serge C. Meimon[a] and Laurent M. Mugnier[a] and Guy Le Besnerais[b]

[a]Office National d'Études et de Recherches Aérospatiales, Département d'Optique Théorique et Appliquée, BP 72, F-92322 Châtillon cedex, France;
[b]Office National d'Études et de Recherches Aérospatiales, Département Traitement de l'Information et Modélisation, BP 72, F-92322 Châtillon cedex, France

ABSTRACT

Current optical interferometers are affected by unknown turbulent phases on each telescope. The complex Fourier samples measured by the instrument are thus multiplied by unknown phasers corresponding to the turbulent differential pistons between each couple of telescopes. So, the only unaffected phase information is the closure phase of each coherent sub-array. Following the radio-interferometry paradigm, we account for the lack of phase information by introducing system aberration parameters, which are structurally analogous to the turbulent differential pistons. Then, we reconstruct the object by minimizing an original criterion in the object and these aberrations.

We have recently designed a metric such that the minimization problem is convex for given aberrations while modeling accurately the noise statistics. The joint criterion is obtained by taking into account the aberrations in this metric. Here, we show how to compute the global minimum of the joint criterion for the aberration step, in spite of the fact that the latter is dramatically non unimodal. This is achieved by exploiting the separable structure of the aberration estimation problem for a known object.

Then, we minimize the by optimizing alternatively the object for the current aberrations and the aberrations for the current object. We are currently testing our technique on experimental data.

Keywords: Imaging, Inverse Problems, Complex visibilities, Closure phase, Interferometry, Optical

1. INTRODUCTION

Optical aperture synthesis allows to reach the angular resolution a hundred meter telescope would provide with several ten meter telescopes. One of the major challenge is to circumvent the turbulence, which corrupts the baseline phases. Until all telescopes are cophased (as in PRIMA[1]), one is led to form closure phases, which remain good observables even in presence of turbulence. However, the number of closure phases is always less than the number of corresponding baseline phases.

The phase information ratio* dramatically increases with the number of telescopes. Unfortunately, most of the current interferometers (VLTI, Keck, IOTA) can't yet provide interferometric samples produced by more than four telescopes. Our work is dedicated to process 3-telescope-interferometers data, which is both the worst case and the basic brick in any optical interferometry imaging algorithms. However, the method can be transposed to more than 3 telescope interferometers data, although it leads to estimate more parameters than needed, and was indeed succesfully used in the IAU- Imaging Beauty Contest (see[2] in this conference).

Radio-astronomers have dealt with interferometric samples with interferometric samples decades before optical interferometrists, due to several orders bigger coherence time or isoplanetic angle. Their work is of course a major source of inspiration for optical interferometry, however to rough a translation leads to unadapted algorithms, since experimental process and errors are very different. Our work can be considered as a carefull adaptation of radio concepts and techniques in the optical setting. With some rephrasing of the goodness-of-fit (data) term, we are able to re-introduce phase calibration parameters and to propose WISARD, an alternating algorithm (over

---

Further author information: <firstname.lastname>@onera.fr
*measurable independent closure phases to unmeasurable baseline phases

objet and phase parameters) in the spirit of self-calibration algorithms proposed by radio-astronomers.[3] After examining the specificities of the optical interferometric data model in section 2, we explain in section 3 how we approximate it. Data are then processed by WISARD, a reconstructor described in section 4, allowing to produce reconstructed maps which are compared to the original objects in section 5.

2. INTERFEROMETRIC SAMPLE DATA

2.1. Complex Visibilities

Coherent arrays   An interferometer can be described as a set of n_a coherent arrays of n_t telescopes observing the same source. For one array i, the measured frequencies are given by

$$\boldsymbol{\nu}^i(j,k) = \frac{\mathbf{r}^i(k) - \mathbf{r}^i(j)}{\lambda},$$

$\mathbf{r}^i(j)$ corresponding to the position of the j$^{\text{th}}$ pupil element of the i$^{\text{th}}$ array, projected on a plane normal to the observation axis.

Object and Fourier bases   The basic observable of an interferometer is the complex visibility, which can be measured from the fringe pattern obtained for each couple of telescopes belonging to the same array. According to the Van Cittert-Zernicke theorem,[4] complex visibilities are related to the sky brightness distribution $X(a,b)$ through a Fourier Transform:

$$V_0\left(\boldsymbol{\nu} = \begin{bmatrix} u \\ v \end{bmatrix}\right) = \iint X(a,b)e^{-2\pi i(ua+vb)}\,\mathrm{d}a\mathrm{d}b \tag{1}$$

a and b being angular positions in the sky and $\boldsymbol{\nu}$ the 2D spatial frequency corresponding to the observable. If the sky brightness $X(a,b)$ is descretized with a cardinal sine object basis in a set of $X_{m,n}$, the integration becomes a finite sum, and equation (1) reads:

$$V_0\left(\boldsymbol{\nu}\right) = \sum_{m,n} X_{m,n}h(m,n,\boldsymbol{\nu}), \tag{2}$$

the $h(m,n,\boldsymbol{\nu})$ being complex coefficients.

Matrix shape   We will abbreviate $V_0(\boldsymbol{\nu}^i(j,k))$ by $V_0^i(j,k)$. If we arrange lexicographically the coefficients $V_0^i(j,k)$ in a vector $\boldsymbol{V}_0$, the coefficients $X_{m,n}$ in a vector $\boldsymbol{X}$ and the coefficients $h(m,n,\boldsymbol{\nu}^i(j,k))$ in a matrix $\boldsymbol{H}$ accordingly to the orders chosen for $\boldsymbol{V}_0$ and $\boldsymbol{X}$, we can reformulate equation (2) in a matrix shape as:

$$\boldsymbol{V}_0(\boldsymbol{X}) = \boldsymbol{H}\boldsymbol{X} \tag{3}$$

2.2. Closure Phases and Visibility Amplitudes

The instantaneous complex visibilities are affected by the atmospheric turbulence through random time-delays at each telescope:

$$V^i(j,k) = V_0^i(j,k)e^{i\left(\alpha^i(k)-\alpha^i(j)\right)} \tag{4}$$

Since the turbulent phasers are not yet measurable, one is led to average short exposure data which are independent of these phasers, such as visibility amplitudes or squared amplitudes, and bispectra, i.e. triple products, into observables. From now on, we will mainly discuss the 3-pupils coherent array case. There are only three pupils $1,2,3$ per triple (i.e. coherent array) i.

Closure phases   Indeed, triple products are the products of three turbulence affected complex visibilities of the same coherent array (i.e. three pupils for which local turbulence is time-coherent). Practically, it corresponds to any set of three complex visibilities measured simultaneously.

For any triple i, with equation (4), we find that the turbulent phasers cancel out[5] in:

$$V^i(1,2)V^i(2,3)V^i(3,1) = V_0^i(1,2)V_0^i(2,3)V_0^i(3,1)$$

A fortiori, the time-averaged bispectra won't be affected by the turbulent phasers either. So the phase of the averaged triple product, called *closure phase*, is measurable independently from the turbulence. We call Cl^i the closure phase obtained for the three pupil 1, 2 and 3 of the array i:

$$Cl^i = \arg V^i(1,2)V^i(2,3)V^i(3,1)$$

With vector notations, the above equation can be written $\boldsymbol{Cl} = \boldsymbol{\Omega}\left(\boldsymbol{V}\right) = \boldsymbol{\Omega}\left(\boldsymbol{V_0}\right) = \boldsymbol{\Omega}\left(\boldsymbol{HX}\right)$, with $\boldsymbol{\Omega}$ the closure operator, defined as the following 1×3 block-diagonal operator: $\boldsymbol{\Omega} = \begin{bmatrix} \omega & 0 & \dots & 0 \\ 0 & \omega & \ddots & \vdots \\ \vdots & \ddots & \ddots & 0 \\ 0 & \dots & 0 & \omega \end{bmatrix}$,

with $\omega = [\arg(.), \arg(.), \arg(.)]$.

We consider in this paper that closure phases are the only phase information available for reconstruction[†].

Visibility amplitudes   Similarly, we can see that the averaged visibility amplitudes $A^i(j,k) = |V^i(j,k)e^{i\left(\alpha^i(k) - \alpha^i(j)\right)}| = |V^i(j,k)|$ are not affected by the turbulence. With vector notations, it reads $\boldsymbol{A} = |\boldsymbol{HX}|$, with $|\boldsymbol{HX}|$ the vector containing the moduli of the coefficients of $\boldsymbol{HX}$.

Visibility phases   It will be useful to define the missing information, i.e. the visibility phases $\varphi^i(j,k) = \arg V^i(j,k)$.

With vector notations, it reads : $\boldsymbol{\varphi} = \arg \boldsymbol{HX}$, with $\arg \boldsymbol{HX}$ the vector containing the arguments of the coefficients of $\boldsymbol{HX}$.

We have seen that we can derive two unaffected quantities from the complex visibilities:

- Visibility amplitudes: $\boldsymbol{A} = |\boldsymbol{HX}|$
- Closure phases: $\boldsymbol{Cl} = \boldsymbol{\Omega}\left(\boldsymbol{HX}\right)$

and that we can't access directly

- Visibility phases: $\boldsymbol{\varphi} = \arg \boldsymbol{HX}$

3. APPROXIMATED STATISTIC MODEL

In this section, we will design a metric which expresses the probability of $\boldsymbol{X}$ in function of the observables and their available statistics.

3.1. Noise statistics/available knowledge

On can reasonably hope that at least standard deviation on visibility amplitudes $\sigma_A^i(j,k)$ and phase closures $\sigma_{Cl}^i(j,k,l)$ will be either supplied or at least computable from other data (e.g. The NPOI and COAST Exchange Format[6] provides standard deviation on squared visibilities and not directly amplitudes). There is much discussion of the noise model for complex visibility, but uncorrelated noises on phase closures and visibility amplitudes seem reasonable.[7]   Moreover, since cross-correlations are not provided, we can't yet use a more refined model.

[†]In multi-spectral interferometry, other phase information such as differential phases can be derived.

3.2. Direct Model

We have shown in section 2 how, for any given $\boldsymbol{X}$, the accordingly vector arranged closures and amplitudes $\boldsymbol{Cl}$ and $\boldsymbol{A}$ can be calculated. Since standard deviation is assumed to be the only available statistics on the various noises we have to consider, we will set all the other momenti of the corresponding distribution laws to zero, i.e, noises are assumed to be uncorrelated zero mean Gaussian. The model consequently reads

$$\begin{cases} \boldsymbol{Cl}_{mes} = \boldsymbol{Cl} + \text{ gaussian noise}(0, \Sigma_{Cl}) \\ \boldsymbol{A}_{mes} = \boldsymbol{A} + \text{ gaussian noise}(0, \Sigma_A) \end{cases} \tag{5}$$

with

$$\begin{cases} \boldsymbol{Cl} = \boldsymbol{\Omega}\,(\boldsymbol{HX}) \\ \boldsymbol{A} = |\boldsymbol{HX}| \\ \Sigma_{Cl} = diag(\sigma_{Cl^i}) \\ \Sigma_A = diag(\sigma_{A^i(j,k)}) \end{cases} \tag{6}$$

Data likelihood would then read $J_1(\boldsymbol{X}) \propto \|\boldsymbol{Cl}_{mes} - \boldsymbol{Cl}\|^2_{\Sigma_{Cl}} + \|\boldsymbol{A}_{mes} - \boldsymbol{A}\|^2_{\Sigma_A}$, with $\|\boldsymbol{U}\|^2_\Sigma = \boldsymbol{U}^t \Sigma^{-1} \boldsymbol{U}$

This is the likelihood considered in the method proposed by Eric Thiébault in Ref..[8] It can be shown that it is not convex[9] and has local minima, which makes minimization more difficult.[10] We show in next subsection how we can recast the problem in a minimization of a joint criterion, depending on the object and on aberration parameters, not convex either, but quadratic in the object, and numerically minimizable in the aberrations.

3.3. Myopic model

The key idea to this point is to consider we virtually measure the set of visibility phases $\boldsymbol{\varphi}$, give or take unknown aberrations $\boldsymbol{\beta}$:

$$\boldsymbol{\varphi}_{mes} = \boldsymbol{\varphi} + \boldsymbol{\beta} + \text{ gaussian noise}(0, \Sigma_\varphi)$$

The following is consistent with the first equation of system (5):

$$\begin{cases} \beta^i(1,2) + \beta^i(2,3) + \beta^i(3,1) = 0 \\ \varphi^i_{mes}(1,2) = \varphi^i_{mes}(2,3) = \varphi^i_{mes}(3,1) = \dfrac{Cl^i_{mes}}{3} \\ \Sigma_\varphi = diag(\sigma_{\varphi^i(j,k)}) \\ \sigma_{\varphi^i(1,2)} = \sigma_{\varphi^i(2,3)} = \sigma_{\varphi^i(3,1)} = \dfrac{1}{3}\,\sigma_{Cl^i} \end{cases} \tag{7}$$

Thus, system (5) is equivalent to:

$$\begin{cases} \boldsymbol{\varphi}_{mes} = \boldsymbol{\varphi} + \boldsymbol{\beta} + \text{ gaussian noise}(0, \Sigma_\varphi) \\ \boldsymbol{A}_{mes} = \boldsymbol{A} + \text{ gaussian noise}(0, \Sigma_A) \end{cases} \tag{8}$$

Data likelihood would then read: $J_2(\boldsymbol{X}) \propto \|\boldsymbol{\varphi}_{mes} - \boldsymbol{\varphi} - \boldsymbol{\beta}\|^2_{\Sigma_\varphi} + \|\boldsymbol{A}_{mes} - \boldsymbol{A}\|^2_{\Sigma_A}$

3.4. Convexifying

Complex variables   We can define $\mathcal{V}(\boldsymbol{X}, \boldsymbol{\beta})$ and $\boldsymbol{V}_{mes}$ such that:

$$\arg \boldsymbol{V}_{mes} = \boldsymbol{\varphi}_{mes} \qquad\qquad \arg \mathcal{V}(\boldsymbol{X}, \boldsymbol{\beta}) = \boldsymbol{\varphi} + \boldsymbol{\beta}$$
$$|\boldsymbol{V}_{mes}| = \boldsymbol{A}_{mes} \qquad\qquad |\mathcal{V}(\boldsymbol{X}, \boldsymbol{\beta})| = \boldsymbol{A}$$

This way, the system (8) reads:

$$\begin{cases} \arg \boldsymbol{V}_{mes} = \arg \mathcal{V}(\boldsymbol{X}, \boldsymbol{\beta}) + \text{ gaussian noise}(0, \Sigma_\varphi) \\ \quad |\boldsymbol{V}_{mes}| = |\mathcal{V}(\boldsymbol{X}, \boldsymbol{\beta})| + \text{ gaussian noise}(0, \Sigma_A) \end{cases} \qquad (9)$$

which can be read as:

$$\boldsymbol{V}_{mes} = \mathcal{V}(\boldsymbol{X}, \boldsymbol{\beta}) + \text{ complex noise}$$

This is a vector *complex* equation. In fact, each line of this vector equality is shaped as:

$$z = z_0 + b,$$

with z, z_0 and b complexes, the modulus and phase of b following two Gaussian laws. But b itself is not a Gaussian noise[‡].

Noise approximations   We have shown[9] that this structure yields a non-convex data-likelihood criterion. This is a specificity of optical interferometry, whereas Radio Imaging deals with circular noise distributions. Although it is possible to use convex circular approximations of the noise distribution,[11] is not adapted when the modulus standard deviation is very different from the phase standard deviation, which is generally the case for optical interferometry. We hence use an elliptic convex approximation,[9] which better fits the noise statistics, as shown in Fig. 1.
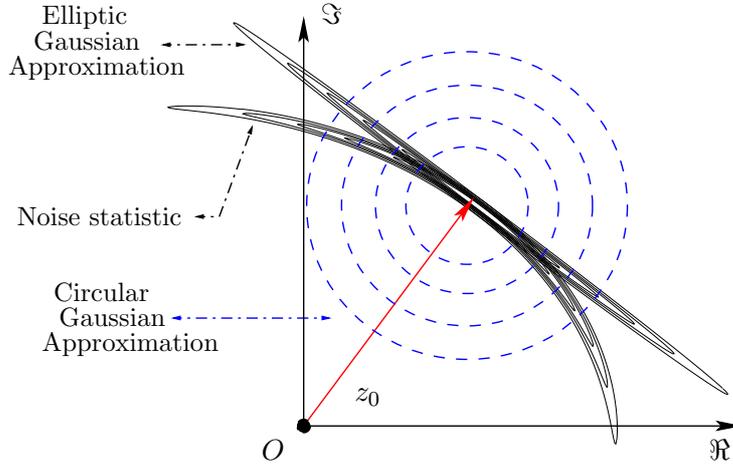

Figure 1. Iso-probable values of z for real and approximated statistics

---

[‡]if b is seen as a vector of $\mathbb{R}^2$, its momenti of orders higher than two are not all null

Criterion Convexification This approximated noise model yields the following data-likelihood criterion:

$$J_{ell}(\boldsymbol{X}, \boldsymbol{\beta}) = \|\boldsymbol{V}_{mes} - \boldsymbol{\mathcal{V}}(\boldsymbol{X}, \boldsymbol{\beta})\|_{C_b}^2 \tag{10}$$

with

$$\|\boldsymbol{U}\|_{C_b}^2 = \begin{bmatrix} \Re(\boldsymbol{U}) \\ \Im(\boldsymbol{U}) \end{bmatrix}^t C_b^{-1} \begin{bmatrix} \Re(\boldsymbol{U}) \\ \Im(\boldsymbol{U}) \end{bmatrix}, \tag{11}$$

C_b being designed from σ_β and σ_A.[9] Let's set $\boldsymbol{\beta}$ to a fixed value. $J_{ell}(\boldsymbol{X}, \boldsymbol{\beta})$ becomes a criterion depending only on $\boldsymbol{X}$: $J_{ell}(\boldsymbol{X}) = \|\boldsymbol{V}_{mes} - \boldsymbol{\mathcal{V}}(\boldsymbol{X})\|_{C_b}^2$. It is a quadratic distance between a known vector $\boldsymbol{V}_{mes}$ and a linearly $\boldsymbol{X}$-dependent quantity:

$$\mathcal{R}(\boldsymbol{\beta}) = \mathrm{Diag}(\exp i\boldsymbol{\beta}) \tag{12}$$
$$\boldsymbol{\mathcal{V}}(\boldsymbol{X}, \boldsymbol{\beta}) = \mathcal{R}(\boldsymbol{\beta})\boldsymbol{H}\boldsymbol{X} \tag{13}$$

It is hence convex and quadratic respect to $\boldsymbol{X}$, so its minimization under positivity constraint or with a linear quadratic prior has been extensively studied and doesn't yield special difficulty.

3.5. Block-splitting aberrations unknowns $\boldsymbol{\beta}$

It can be easily shown that the criterion $J_{ell}(\boldsymbol{X}, \boldsymbol{\beta})$ divides in "split criteria", each one accounting for the measurements obtained with the ith triple of telescopes:

$$J_{ell}(\boldsymbol{X}, \boldsymbol{\beta}) = \sum_{i=1...n_a} J_{ell}^i(\boldsymbol{X}, \boldsymbol{\beta}^i(1,2), \boldsymbol{\beta}^i(2,3), \boldsymbol{\beta}^i(3,1)), \tag{14}$$

This is a consequence of the fact that we deal with statistically independent triples of telescopes observing the same object. So one aberration parameter, which accounts for turbulence, affects only one triple, whereas the object distribution is present in all the measurements.

In fact, the functional $J_{ell}(\boldsymbol{\beta}) = \sum\limits_{i=1...n_a} J_{ell}^i(\boldsymbol{\beta}^i(1,2), \boldsymbol{\beta}^i(2,3), \boldsymbol{\beta}^i(3,1))$ is splitted in functions of only 2 independent parameters $\boldsymbol{\beta}^i(1,2)$ and $\boldsymbol{\beta}^i(2,3)$, which can be minimized separately. Indeed, $\boldsymbol{\beta}^i(3,1)$ can be deduced from the two others with equation (7).

3.6. Final metric

We have re-introduced aberration parameters which account for the missing phase information, and approximated the noise statistics. This way, we have expressed the problem through a joint criterion, which is quadratic in the object, and globally optimizable in the aberrations. It seems therefore natural to minimize this criterion by alternating object optimization steps with given aberrations and aberration optimization steps with given object, which is a technique inherited from the "self-calibration" alternating algorithmic structure used in radio-astronomy. In other words, we have carefully recast the problem as the one solved in radio-astronomy, while accurately fitting the optical model specificities.

4. WISARD, AN ALTERNATING RECONSTRUCTOR

In this section, we describe our interferometric data reduction algorithm, WISARD, standing for Weak-phase (i.e. 3 or 4 pupil array cases) Interferometric Sample Alternating Reconstruction Device.

4.1. Object priors

Due to the poor spectral coverage, the object reconstruction, even with known aberrations, is an ill-posed inverse problem and must be regularized (see Refs.[12] and[13] for reviews on regularization), in the sense that some *a priori* information must be introduced in their resolution for the solution to be unique and robust to noise. Since long base interferometer reach resolutions never achieved before, reliable models of objects at this scale are not always available.

Yet, positivity of the pixels can always be imposed. So all minimization are performed under constraint of positivity. We also use a circularized version of the result obtained without prior knowledge (besides the positivity constraint) as a Power Spectral Density (PSD) model.[14] We will therefore minimize the following criterion:

$$J(\boldsymbol{X}, \boldsymbol{\beta}) = J_{ell}(\boldsymbol{X}, \boldsymbol{\beta}) + J_{prior}(\boldsymbol{X})$$

under positivity constraint, $J_{prior}(\boldsymbol{X})$ being a quadratic function accounting for the PSD model, and $J_{ell}(\boldsymbol{X}, \boldsymbol{\beta})$ the data-likelihood criterion described in previous section.

4.2. Progressive use of the data

We have witnessed during preliminary tests of WISARD that good low frequencies reconstruction is crucial. If the global structure of the object is retrieved, the higher frequency components are likely to be reconstructed as well. It seems therefore natural to perform a first reconstruction with only the low frequency data, and then add progressively the remaining data. To blend correctly the data into the minimizer, it's crucial not to break the triples: aberrations are calibrated following a closure condition which links the baseline measurements 3 by 3. We start the minimization with a set of low spatial frequency measurements, isotropic enough to preserve the global structure of the object, and small enough to filter the high frequencies. This set is selected by maximizing an isotropy metric, penalized by the number of frequencies of the set. We're currently working on simplifying this step.

4.3. Alternating Optimization

Although the criterion we have designed is convex for given aberrations, it is not convex for the whole unknown set, i.e. for both aberrations and object. Anyway, a more comprehensive study of its behavior is in progress.

To minimize it, we use an alternating pattern, i.e. we optimize it with given aberrations respect to the object, and then optimize the aberrations with a given object.

Object step The object step is a convex functional minimization under positivity constraint. It is performed by a BFGS-method (Broyden-Fletcher-Goldfarb-Shanno) software OP-VMLM, designed by Eric Thiébaut[§] .

The functional contains a quadratic regularization term computed from the PSD model. The hyper-parameter is currently set to 1. We are working on a more sophisticated regularization strategy, but we try to keep the number of user-defined parameters as close to 0 as possible.

Aberration step To this point, we have to find the global minimum of

$$J_{ell}(\boldsymbol{\beta}) = \sum_{i=1...n_a} J_{ell}^i \left(\boldsymbol{\beta}^i(1,2), \boldsymbol{\beta}^i(2,3), \boldsymbol{\beta}^i(3,1) \right).$$

As previously mentioned, it can be done by finding for all i the $\boldsymbol{\beta}^i(1,2), \boldsymbol{\beta}^i(2,3), \boldsymbol{\beta}^i(3,1)$ such that $J_{ell}^i \left(\boldsymbol{\beta}^i(1,2), \boldsymbol{\beta}^i(2,3), \boldsymbol{\beta}^i(3,1) \right)$ is minimum. If we recall $\beta^i(1,2) + \beta^i(2,3) + \beta^i(3,1) = 0$ from system (7), we

---

see that there are in fact only two independent unknowns $(\boldsymbol{\beta}^i(1,2), \boldsymbol{\beta}^i(2,3))$. We can then calculate the value of each "split criterion" J^i_{ell} for, say, a hundred values of each of the parameters, spanning $[0, 2\pi] \times [0, 2\pi]$ (Fig. 2), and thus locate the global minimum give or take a hundredth of 2π. The split criterion restricted to this $2\pi/100 \times 2\pi/100$ is very likely to be unimodal, so a local descent algorithm can be used to refine the estimation of the parameters.
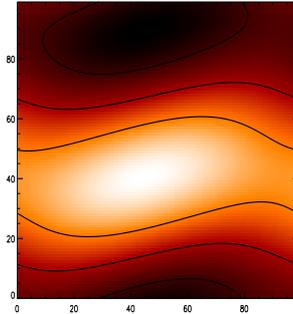
Figure 2. Behavior of a split criterion in function of the two corresponding aberration parameters

Initialization   Aberrations are initially set to zero, and the start object is a centered Gaussian circular object which parameters are fit according to squared visibility data. Since reconstruction is shift-invariant, this helps centering the reconstruction.

5. AN INTERFEROMETRY IMAGING BEAUTY CONTEST

We took part to an international blind reconstruction contest, which was aimed to compare the performances of five different algorithms designed for synthesis imaging. In this section, we recall the results submitted to this contest. For more information, see.[2]

5.1. Data sets

This subsection is taken form Lawson et. al[2]: The data sets have been produced by Christian Hummel, using the data reduction software OYSTER[¶] and simulating a six-station Navy Prototype Optical Interferometer (NPOI). The image of the star with asymmetric shell shown in Fig. 3 was provided to Christian by Peter Tuthill. The double star data described in Fig. 4 was simulated within OYSTER. The noise is simulated Poisson noise in 2 ms fringe frames. The errors are not correlated. The simulated measurements were reduced to yield the contest data in exactly the same way that real data would have been processed.

5.2. Results

As shown in Fig. 5, we have retrieved satisfactorily the global structures of both objects. However, the central dot on the first data set object has not been successfully reconstructed. This is due for one part to the lack of high frequency measurements in a diagonal direction (bottom-left to upper-right): the dot is correctly resoluted in the other diagonal direction, where high frequency measurements are available. On the other hand, the quadratic regularization tends to flatten the small details of the objects.

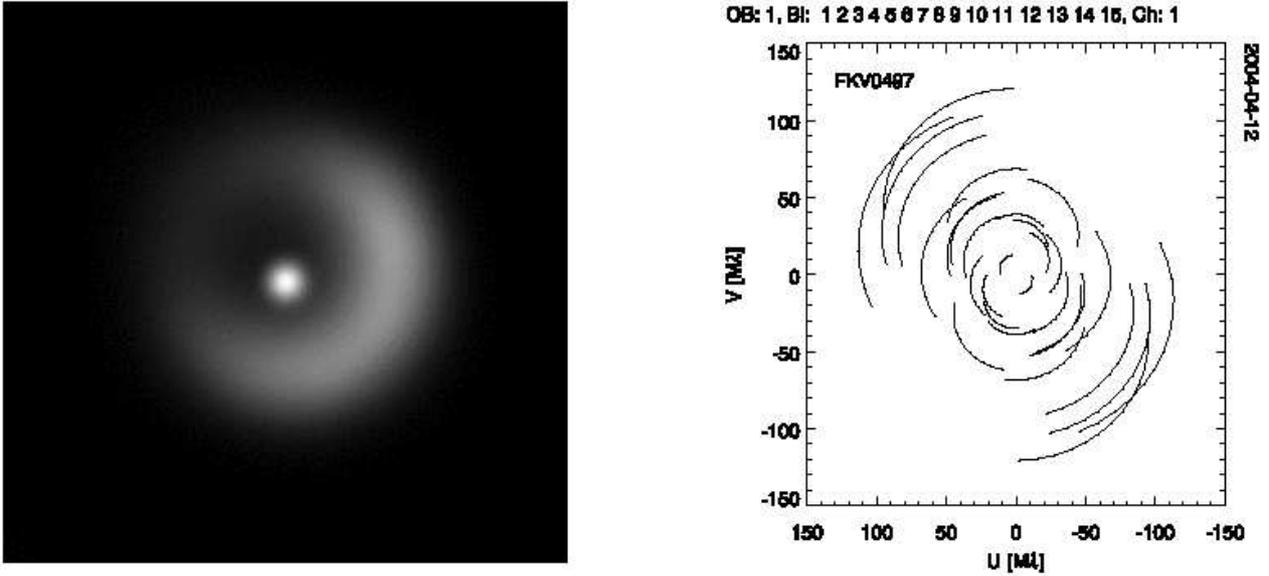[¶]see http://www.sc.eso.org/~chummel/oyster/oyster.html

Figure 3. The source file for Data Set 1 and the u-v plane coverage used to sample the model. A model of LkHa 101, was provided in FITS format by P.G. Tuthill. The 242 × 242 pixel image was sized with pixels of 0.05 mas on a side and sampled with a simulated six-station Navy Prototype Optical Interferometer (NPOI). About half of the data points are in the low signal-to-noise regime.
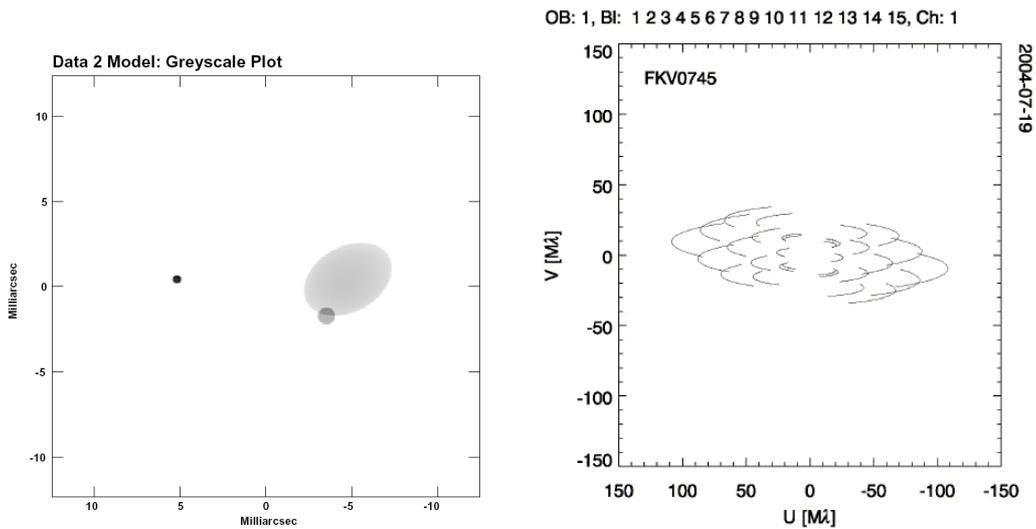

Figure 4. The source file for Data Set 2 and the u-v plane coverage used to same the model. A double star was simulated within OYSTER. The u-v coverage for a six-station NPOI array is shown on the right. Most of the data points are in the high signal-to-noise regime.

6. FUTURE WORK

Although the reconstructed maps are satisfactory, since the global structure of the objects are preserved, we hope to get even closer by adapting WISARD to more-than-3-telescope arrays. This will help reducing the total number of aberration parameters to estimate, but each split criterion will depend on more than two parameters,
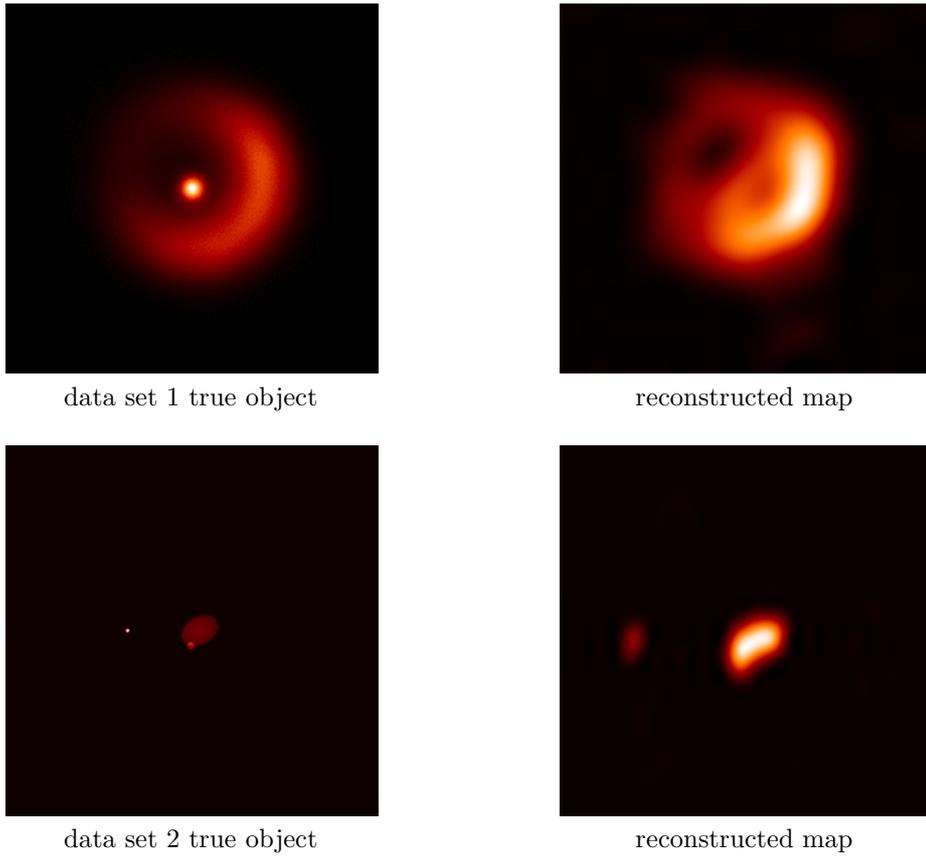
data set 1 true object   reconstructed map

data set 2 true object   reconstructed map

Figure 5. Original objects and reconstructions

which will make it more difficult to minimize. Another crucial aspect is the extensive study of the criterion shape, e.g. its behavior in function of the uv-coverage, the object prior, the kind of object, etc... Finally, we are currently working on different regularization methods.

REFERENCES

1. A. Quirrenbach *et al.*, "Prima: Study for a dual beam instrument for the vlt interferometer,"
2. P. R. Lawson *et al.*, "An interferometric imaging beauty contest," in *New frontiers in stellar interferometry*, **5491**, 2004.
3. Thompson, Moran, and Swenson, *Interferometry and synthesis in Radio-astronomy*, Krieger Pub. Co., 1984.
4. J. W. Goodman, *Statistical optics*, John Wiley & Sons, New York, 1985.
5. F. Roddier, "Triple correlation as a phase closure technique," *Opt. Commun.* **60**(3), pp. 145–148, 1986.
6. T. Pauls *et al.*, "A data exchange standard for optical (visible/ir) interferometry," in *New frontiers in stellar interferometry*, **5491**, Proc. Soc. Photo-Opt. Instrum. Eng., 2004.
7. "http://www.mrao.cam.ac.uk/~jsy1001/exchange/complex/complex.htm."
8. L. Delage, F. Reynaud, and E. Thibaut, "Imaging laboratory test on a fiber linked telescope array," *Opt. Commun.* **160**, pp. 27–32, Feb. 1999.
9. S. Meimon, L. Mugnier, and G. Le Besnerais, "Approximations convexes de criteres pour la synthese de Fourier optique," in *19ime Colloque sur le Traitement du Signal et des Images*, J.-M. Chassery and C. Jutten, eds., GRETSI, Sept. 2003.
10. W. Press, B. Flannery, S. Teukolsky, and W. Vetterling, *Numerical Recipes in C*, Cambridge University press, 1988.
11. A. Lannes, "Weak-phase imaging in optical interferometry," *J. Opt. Soc. Am. A* **15**, pp. 811–824, Apr. 1998.
12. D. M. Titterington, "General structure of regularization procedures in image reconstruction," *Astron. Astrophys.* **144**, pp. 381–387, 1985.
13. G. Demoment, "Image reconstruction and restoration: Overview of common estimation structures and problems," *IEEE Trans. Acoust. Speech Signal Process.* **37**, pp. 2024–2036, Dec. 1989.
14. J.-M. Conan, L. M. Mugnier, T. Fusco, V. Michau, and G. Rousset, "Myopic deconvolution of adaptive optics images using object and point spread function power spectra," **37**, pp. 4614–4622, July 1998.